Testing and Isolation Efficacy: Insights from a Simple Epidemic Model

June 9, 2021

1 Abstract

[**BMB:** *abstract needs another editing pass, skipping for now*]

The effect of testing processes, including testing and test reporting, on epidemic dynamics, involving infection and recovery, can be studied at the individual level or the community level (e.g., nursing homes, long-term-care facilities, etc.). Gaining insights to determine the sensitivity of the epidemic dynamics with respect to the testing processes will depend on underlying factors including the level of focus (individual or community), assumptions (model), and the interplay between these factors. In particular, fast testing and test reporting may be beneficial at the community-level, supported by many studies, as it gives a rapid assessment of the situation, identifies hot spots, and may enable rapid contact-tracing. However, the potential advantage of a slow rate of test return on the dynamics of an epidemic is real, often neglected, and needs to be quantified. At the individual level, this advantage can manifest in the following sense: individuals awaiting their test results or who have tested positive may partially or fully self-isolate, thus reducing or eliminating their potential in the transmission process. In this paper, we investigated this individual-level effect of testing processes on the epidemic dynamics by developing a SIR-type model. Although the model development was motivated by the COVID-19 epidemic, the model has general epidemiological and testing structures. The realistic components of the model include *per capita* testing intensity, test sensitivity and specificity, rate of test return, and isolation efficacy (i.e., reduction of the transmission probability by isolating individuals). The novel component is the compartment-specific relative testing weights, which reflect the testing strategies — surveillance, diagnosis, or control. Here, we compare two testing strategies, random vs. targeted, and concluded that increasing testing "focus" from random to targeted always decreases $\mathcal{R}_0$. Further, the following processes always decreases $\mathcal{R}_0$; increasing the isolation efficacy parameters for tested and confirmed individuals, higher testing intensity if testing is random or testing intensity is small, and a higher rate of test return if the isolation efficacy for tested-awaiting individuals is low.

2 Introduction

The observed dynamics of the COVID-19 epidemic have been driven both by epidemiological processes (infection and recovery) and by testing processes (testing and test reporting). In addition to shaping epidemic observations (via case reports), testing processes also alter epidemiological dynamics. Because individuals with confirmed infections (positive tests) are likely to self-isolate, and individuals who are awaiting the results of a test may also do so (possibly to a lesser extent), testing will generally increase the number of people who are isolating and hence reduce epidemic growth rates. We developed a mechanistic model that incorporates epidemic processes and testing in order to explore the effects of testing and isolation on epidemic dynamics.

If testing influences behavior, then epidemic dynamics will depend on who gets tested. The impacts of testing will depend both on testing intensity (tests performed per day) and on how strongly testing is focused on people who are infectious. This level of focus depends in turn on the purpose and design of testing programs. When testing is done for the purposes of disease surveillance (Foddai et al., 2020) tests are typically assigned randomly (or using a stratified random design) across the population in order to make an unbiased assessment of population prevalence.

Over the course of the COVID-19 pandemic, however, the vast majority of testing has been done with other goals – primarily diagnostic (determining infection status for clinical purposes), or for control (determining infection status in order to isolate cases that have been found by contact tracing), which we characterize as *targeted* testing strategies. In these cases, testing probabilities vary widely across epidemiological compartments; in our dynamical model, we will characterize these probabilities by assigning a *per capita* testing weight to each compartment that determines the *relative* probability that an individual in that compartment will be selected for testing (see Methods).

Diagnostic testing focuses on people with infection-like symptoms; thus the relative testing weights for infected people will depend on the relative probability of infected people having symptoms. For COVID-19 infection, the testing weights will depend on the proportion of asymptomatic infections, the time spent pre-symptomatic vs. symptomatic during the course of an infection, and on the incidence of COVID-19-like symptoms among people in the population *not* infected with COVID-19. Testing for epidemic control focuses on known contacts of infected people; in this case the testing weights for infected vs. uninfected people will depend on the probability of infection given contact, as well as the effectiveness of the system for identifying suspicious contacts.

As epidemiologists, we want to know whether an epidemic will initially grow exponentially following its introduction in a susceptible population. In mathematical epidemiology, we determine this outcome by studying the basic reproduction number $\mathcal{R}_0$, defined as the expected number of secondary infections arising from a typical infective individual in a completely susceptible population (Dietz, 1993). In the early stages of an epidemic the number of infected individuals is expected to grow exponentially over time when $\mathcal{R}_0 > 1$. Although the value of $\mathcal{R}_0$ cannot completely characterize the dynamics of even the simplest epidemic model (Shaw and Kennedy, 2021), it does give a simple and widely accepted index for the difficulty of control, as well as an indication of the likely final size of an epidemic (Ma and Earn, 2006).

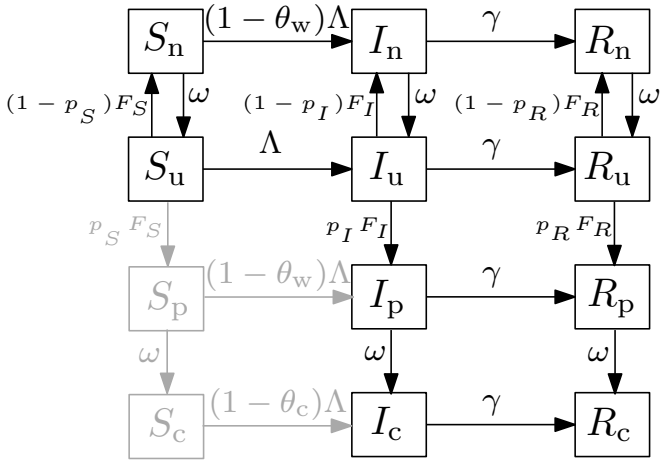

Figure 1: Flowchart of the SIR (Susceptible-Infectious-Recovered) model, A1. The disease-based status of a compartment X ($X \in \{S, I, R\}$) is combined with the testing status including X_{u}, X_{p}, X_{n} and X_{c}, for *untested*, waiting-for-*positive*, waiting-for-*negative*, or *confirmed positive*, respectively. The force of infection is denoted by Λ (Eq. (3)); γ is the recovery rate; ω is the rate of test return; and F_X (Eq. (2)) and p_X represent the *per capita* testing rate and the sensitivity (probability of positive tests), respectively, for compartment X. For further description of the parameters see Table 1. Note that there is a slight mismatch in the top-to-bottom order of the testing-based compartments of each disease-based compartment X between this flowchart and the model equations (A1); here we have switched X_{u} and X_{n} for visual clarity.

In order to understand the effect of testing processes on an epidemic dynamics, we developed a mechanistic SIR-type model with epidemic and testing components. This model provides a sensible platform to link the modeling of epidemic and testing components and study their interaction. Here, we studied the the effect of testing intensity, rate of test return and the isolation efficacy in reduction of the probability of transmission on the epidemic dynamics when different levels of testing focus (from random to highly targeted) are in place.

3 Methods

We developed a deterministic model, Eqs. (A1), which groups individuals based on disease status and testing status. Disease states include Susceptible, Infectious and Recovered; testing status categorizes people as *untested*, waiting-for-*positive*, waiting-for-*negative*, or *confirmed positive* (Fig. 1). The testing status of an individual in a given disease compartment X (where $X \in \{S, I, R\}$) is denoted by a subscript, namely X_{u}, X_{p}, X_{n} and X_{c}, for *untested*, waiting-for-*positive*, waiting-for-*negative*, or *confirmed positive*, respectively. Further, two 'accumulator' compartments, N and P, are included in order to collect cumulative reported negative or positive tests. The model equations and details of calculation of the basic reproduction number $\mathcal{R}_0$ are presented in the appendix (Sec. A.1).

Table 1 defines the model parameters, which are generally *per capita* flows between compartments, or modifiers to these flow rates. The novel component of the model lies in the compartment-specific relative testing weights w_S, w_I and w_R; these give the relative rates at

which people in the S, I, and R compartments are tested, respectively. Thus, we can specify different levels of testing focus from random (all weights equal) to highly targeted (higher weights in more intensively tested compartments). For example, $w_I/w_S = 3$ means that infected individuals are tested at three times the *per capita* rate of susceptible individuals.

In order to allow parameterization of the model by the total (overall) *per capita* testing rate, we define the weighted size of the testing pool $W = w_S S_\mathrm{u} + w_I I_\mathrm{u} + w_R R_\mathrm{u}$, and calculate a scaling parameter for testing as:

$$\sigma = \frac{\rho N_0}{W}, \tag{1}$$

where ρ is the *per capita* testing intensity for the population, defined as the number of daily tests administered in a population of size N_0. Thus, the *per capita* testing rate for compartment X is

$$F_X = \sigma w_X, \quad \text{where} \quad X \in \{S, I, R\}. \tag{2}$$

For a highly sensitive test, infected people typically flow through to the "confirmed positive" (I_c, R_c) compartments and are thus unavailable for further testing. Over the course of the epidemic, a sufficiently large fixed testing rate as specified in (1) can exhaust the pool of people available for testing, leading to a singularity when too few people are left untested to support the specified rate. Although this phenomenon does not affect our analysis of $\mathcal{R}_0$, it can affect the temporal dynamics (in the appendix we present an adjustment to the model that solves this problem).

The classical SIR model assumes a well-mixed population; homogeneity of the population (i.e., all individuals are equally susceptible and equally infectious with the same recovery rate when infected); exponentially distributed duration of infection; and large population size (Keeling and Rohani, 2011). In addition to these standard assumptions, our model assumes:

(i) there is a single force of infection (new cases per unit time), Λ, defined as

$$\Lambda = \frac{\beta}{N_0}\big(I_\mathrm{u} + (1-\theta_\mathrm{w})(I_\mathrm{n} + I_\mathrm{p}) + (1-\theta_\mathrm{c})I_\mathrm{c}\big), \tag{3}$$

with transmission rate β; θ_w is the isolation efficacy (reduction of the probability of transmission) for individuals waiting for test results, while θ_c is the isolation efficacy for individuals who have received a positive test ("confirmed positive": Table 1). Susceptible individuals who are waiting for test results experience an additional transmission factor of $1 - \theta_\mathrm{w}$ (Fig. 1).

(ii) confirmed-positive individuals isolate more effectively than those awaiting test results, i.e.

$$0 \le \theta_\mathrm{w} \le \theta_\mathrm{c} \le 1.$$

For simplicity we assume that tests are perfectly *specific* — uninfected individuals never test positive ($p_s = 0$). Thus there are no waiting-for-positive or confirmed-positive susceptible individuals (we assume that these states are also absent from the initial conditions, i.e. $S_\mathrm{p}(0) = S_\mathrm{c}(0) = 0$), which reduces the number of model states from 12 to 10.

Symbol	Description	Unit	Value
N_0	Total population size	people	10^6
ω	Rate of test return, i.e., rate of onward flow from "waiting" to "confirmed" or "untested" compartments	1/day	-
γ	Recovery rate	1/day	1/6
ρ	*per capita* testing intensity	1/day	-
θ_{w}	Isolation efficacy (reduction of the transmission probability) for "waiting" individuals	-	-
θ_{c}	Isolation efficacy for "confirmed positive" individuals	-	-
β	Transmission rate	1/day	0.5
Λ	Force of infection	1/day	-
p_S	Probability of positive tests for S $(= 1 - \text{specificity})$	-	0
p_I	Probability of positive tests for I $(=$ sensitivity$)$	-	1
p_R	Probability of positive tests for R $(= 1 - \text{specificity})$	-	0.5
w_S, w_I, w_R	Relative testing weights	-	Random: $\{1, 1, 1\}$ Targeted: $\{0.3, 1, 1\}$

Table 1: Parameters of the model (A1).

The Disease-Free Equilibrium (DFE) for the SIR model (Eqs. A1) is found by setting the infected compartments to 0 and solving for the unknowns. The DFE is

$$S_{\mathrm{n}}^{*} = \frac{\rho}{\omega} N_0,\ S_{\mathrm{u}}^{*} = \frac{\omega - \rho}{\omega} N_0, \text{ and } I_j = R_j = 0 \text{ for all } j. \tag{4}$$

The corresponding *per capita* testing rate (Eq. 2) for the infected compartment I at DFE is one of the key analysis parameters and can be simplified as

$$\hat{F}_I = (\omega\rho/(\omega - \rho))w_I/w_S \quad . \tag{5}$$

The basic reproduction number, $\mathcal{R}_0$, was calculated by using the next-generation matrix method (van den Driessche and Watmough, 2002). We present $\mathcal{R}_0$ as

$$\mathcal{R}_0 = \frac{\beta}{\gamma}\left(1 - \Delta\right), \tag{6}$$

where the term β/γ is the classical basic reproduction number for a SIR model without testing and isolation (Keeling and Rohani, 2011), and $\Delta > 0$ is the effectiveness of control due to testing and isolation processes defined as

$$\Delta = \frac{1}{CN_0}\big(C_1 S_{\mathrm{u}}^{*} + (C_2(1 - \theta_{\mathrm{w}}) + C\theta_{\mathrm{w}})S_{\mathrm{n}}^{*}\big), \tag{7}$$

where

$$C = (\omega + \gamma)\Big(\gamma(\omega + \gamma) + (\gamma + \omega p_I)\hat{F}_I\Big), \tag{8}$$

$$C_1 = (\omega + \gamma)(\theta_{\mathrm{w}}\gamma + \theta_{\mathrm{c}}\omega p_I)\hat{F}_I, \tag{9}$$

$$C_2 = \Big(\omega\gamma(1 + p_I)\hat{F}_I + \gamma^2(\omega + \gamma + \hat{F}_I)\Big)\theta_{\mathrm{w}} + \omega^2 p_I \hat{F}_I \theta_{\mathrm{c}}. \tag{10}$$

(Appendix A.1 gives a detailed derivation of these expressions). The explicit formula of $\mathcal{R}_0$ enables us to study the effects of testing and isolation parameters on $\mathcal{R}_0$ both analytically and via numerical solutions. We are specifically interested in parameters that could be manipulated by public health policy: isolation efficacy, θ_{c} and θ_{w}; *per capita* testing intensity, ρ; and the rate of test return, ω. In particular, we look at the partial derivatives of Δ with respect to these parameters (App. A.2). We derived general expressions for these derivatives. However, we analyzed the effect of ω on $\mathcal{R}_0$ for the special case of low testing intensity. Specifically, by making the restriction $\rho \ll 1$, we are able to Taylor-expand Δ at $\rho = 0$, use the linear approximation with respect to ρ and analyze the resulting simplified derivatives to illustrate a surprising non-monotonic relationship between $\mathcal{R}_0$ and ω.

The computations in this paper, specifically, calculation of the next-generation matrix and simplification of the $\mathcal{R}_0$ expression, were performed in Maple™ (Maple, 2010). We used R (R Core Team, 2020) for numerical solutions, in particular for plotting the contours of Δ (Eq. (7)) over a range of parameters. We computed the values and contours of Delta at both low (Fig. 2) and high (Fig. 3) testing intensities, and for both random testing ($w_S = w_I = w_R = 1$) and targeted testing ($w_S = 0.3$; $w_I = w_R = 1$).

The low-testing case Fig. 2 reflects the case where ρ is small relative to the population size. Specifically, $\rho \in [0, 0.013]$, and test return rate $\omega \in [1/12, 2]$. This testing intensity reflects realistic testing rates during the COVID-19 pandemic, i.e. a maximum of 1.3% of the population per day, giving a maximum of 10000 tests/day in a population of size $N_0 = 10^6$ (this is approximately four times the maximum testing rate in Ontario, Canada in mid-2021). The less realistic high-testing case Fig. 3 is included to highlight the occurrence of non-monotonic changes in $\mathcal{R}_0$ with respect to ρ. In Fig. 3 the maximum capacity of ρ is larger relative to the population size, $\rho \in [0, 1/5)$ and the test return rate $\omega \in [1/5, 2]$; these values are clearly unrealistic for a large population but might be relevant for some population undergoing focused testing, such as a sports league or university. The critical contour of $\Delta = 1 - \frac{\gamma}{\beta}$, corresponding to the threshold $\mathcal{R}_0 = 1$, is shown as a dotted line in Fig. 2 and Fig. 3; combinations of ρ and ω that lie above this critical contour will control the epidemic. The implied baseline value of $\mathcal{R}_0 = \frac{\beta}{\gamma}$ in these figures is 3, corresponding to a case where the epidemic spreads slowly even in the absence of testing and tracing.

4 Results

We can use the formula for $\mathcal{R}_0$ (6) to make a number of straightforward conclusions about parameters whose effects on $\mathcal{R}_0$ are monotonic, i.e. when the partial derivative of Δ has a consistent sign (Appendices A.2, A.3, A.5).

1. Increasing isolation efficacy for waiting (θ_{w}) and confirmed-positive (θ_{c}) individuals always decreases $\mathcal{R}_0$ (Eqs. A13, A16, A18);

2. Higher testing intensity ρ decreases $\mathcal{R}_0$ if testing is random (all w_X equal) or testing intensity (ρ) is small (Eq. A20).

3. Increasing the rate of test return (ω) always decreases $\mathcal{R}_0$ if waiting individuals do not isolate ($\theta_w = 0$) (Eq. A23).

4. Increasing testing focus, i.e. changing the testing weights from random ($w_S = w_I$) toward targeted ($w_S < w_I$), always decreases $\mathcal{R}_0$ (Eq. A24).

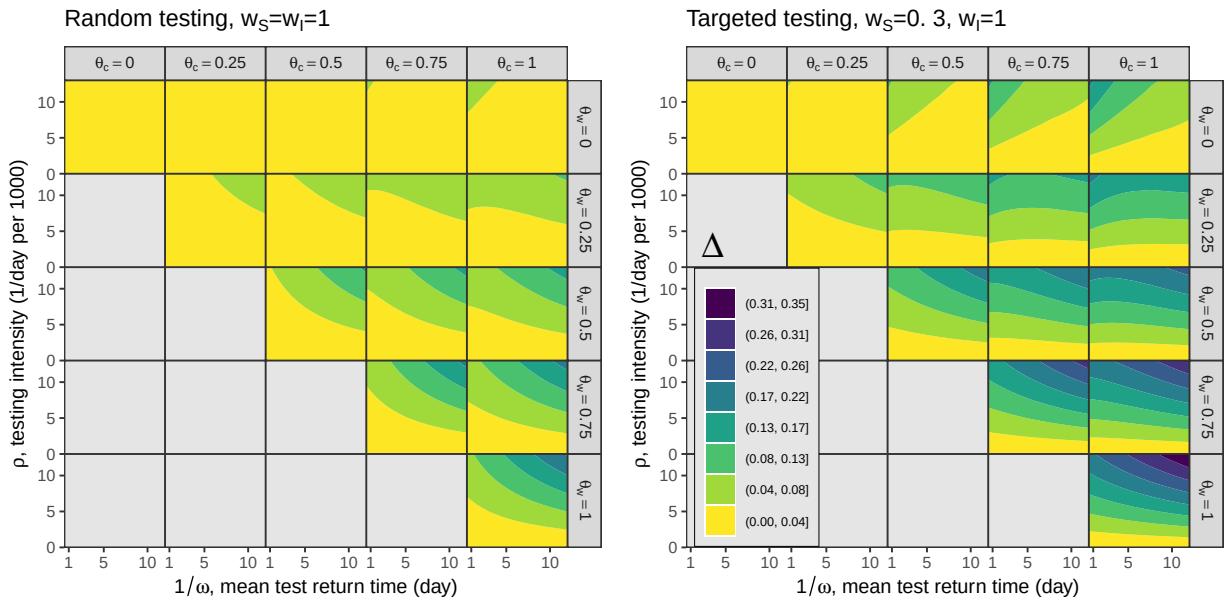

(a) (b)

Figure 2: **Effectiveness of testing and isolation in reducing $\mathcal{R}_0$ at low *per capita* testing intensity.** Numerical evaluation of the effectiveness of control (Δ: eq. A.2), over a range of testing and isolation parameters. Parameter values (Table 1): $\beta = 0.5$ 1/day, $1/\gamma = 6.0$ days (baseline $\mathcal{R}_0 = 3.0$, $r = 0.3$); $\omega \in [1/12, 2]$ 1/day; $\rho \in [0, 0.013]$ 1/day per capita; θ_w and θ_c vary between 0 (no effect of isolation) and 1 (complete elimination of transmission); $p_S = 0$, $p_I = 1$ and $p_R = 0.5$. Only parameter sets where $\theta_c \geq \theta_w$ (confirmed-positive individuals isolate more effectively than waiting individuals) are shown; the alternative case, $\theta_w > \theta_c$, is unrealistic. Contours of Δ are plotted for (a) random testing ($w_S = w_I = w_R = 1$) and (b) targeted testing ($w_S = 0.3$; $w_I = w_R = 1$).

However, there are also two specific cases where Δ changes non-monotonically, in counterintuitive directions, as a function of testing and isolation parameters.

- We would generally expect increasing testing delays to increase $\mathcal{R}_0$, thus decreasing effectiveness of control Δ. This is in fact what happens when waiting individuals do not isolate ($\theta_w = 0$, top row of Fig. 2) — as we move to the right within each plot in this row, Δ decreases. However, when waiting individuals isolate ($\theta_w > 0$), we more often see the opposite effect: longer testing delays lead to a greater control effect Δ. This is because people waiting for negative tests are assumed to continue to isolate; this applies both to susceptibles and to people who became infected while waiting for negative test results. This effect outweighs the effect of confirmed individuals isolating except when this isolation parameter θ_c is substantially bigger than θ_w. This result depends on the idea that, all else equal, people who have to wait longer for test results isolate at the same level (but for a longer time) as they would if the wait were shorter.

- Fig. 2 also shows that greater testing intensity (increasing ρ) generally increases the effectiveness of control (moving up in each panel). This relationship can be reversed, however, at very high testing intensities. This can only occur when testing is targeted,

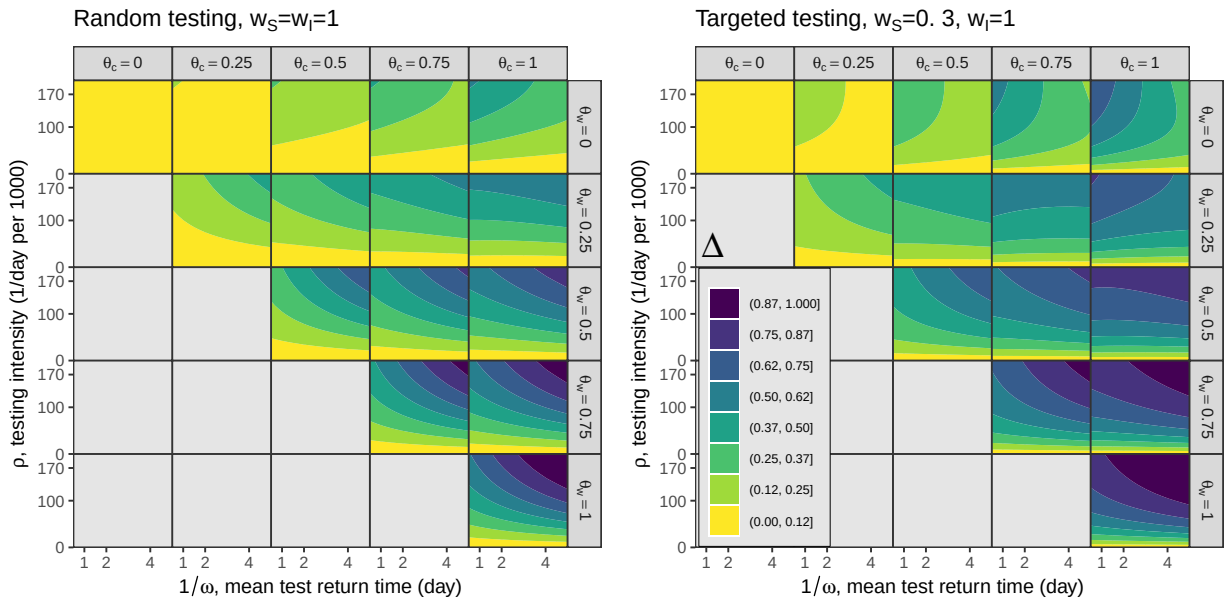

(a) (b)

Figure 3: **Effectiveness of testing and isolation in reducing $\mathcal{R}_0$ at high *per capita* testing intensity.** Numerical evaluation of the effectiveness of control (Δ: eq. A.2), over a range of testing and isolation parameters. Parameters as in Fig. 2 except: $\omega \in [1/5, 2]$ 1/day, $\rho \in [0, 1/5)$ 1/day. As in Fig. 2, subplots show (a) random testing where $w_S = w_I = w_R = 1$ and (b) targeted testing where $w_S = 0.3$ and $w_I = w_R = 1$.

and θ_w is relatively small (Fig. 3(b), right three panels of top row). It is theoretically possible for increasing testing intensity to *increase* $\mathcal{R}_0$ because more rapid testing leaves more susceptibles in the "waiting-for-negative-results" category at the DFE; if these people become infected while waiting, they will need to wait for their negative test result before they can be tested again, receive a positive test, and then begin self-isolating. This effect is usually weak compared to the beneficial effects of testing.

5 Discussion

In this paper, we have defined and analyzed a simple compartmental model that combines epidemiological dynamics (as defined by a simple SIR model) with the dynamics of testing and isolation. Our model is a caricature — it models the most basic feedbacks between epidemic and testing processes, but does not attempt to incorporate the many known complications of COVID-19 epidemiology (e.g. exposed, presymptomatic, and asymptomatic compartments [REFS][**Ali:** *(Kain et al., 2021) OK?*]; time-varying testing rates [REFS?]; behavioural dynamics [REF Weitz/Park/Dushoff] [**Ali:** *(Weitz et al., 2020) OK?*]). Thus, it is most appropriate for assessing the *qualitative* phenomena that arise from the interactions between epidemiology and testing, rather than for making quantitative predictions or guiding pandemic responses.

Many of the qualitative results we have derived are mathematical confirmations of simple,

common-sense intuitions. In particular, we can generally decrease $\mathcal{R}_0$ by increasing isolation efficacy or testing intensity; returning tests faster, if individuals do not isolate while they are waiting for results; or increasing testing focus to target individuals who are likely to be infectious (e.g. symptomatic people or close contacts of known infections).

However, we did find two surprising trends: longer delays in returning tests can decrease the spread of the epidemic, and increasing testing rates can increase its spread.

Over a broad range of parameter space (for random testing, approximately $\theta_w \geq 0.25$; for targeted testing, $\theta_w \geq 0.25$ and either $\theta_c \geq 0.5$ or $1/\omega > 5$), decreasing ω — i.e., decreasing the rate at which tested people find out about their infection status — decreases $\mathcal{R}_0$. This result is counterintuitive; public health agencies have invested a lot of effort in increasing this rate. Dynamically, this effect occurs because speeding up test returns shortens the isolation period of uninfected individuals. For infected people it only shortens the time to progression to the isolation level of the confirmed-positive compartment. Slowing test returns increases $\mathcal{R}_0$ only if the proportion of infectives in the tested population (test positivity), and the magnitude of increase in isolation effectiveness from the waiting to the confirmed-positive compartment, are large enough to outweigh the decrease in isolation of uninfected waiting individuals.

While slowing test returns does decrease $\mathcal{R}_0$ over a broad range of parameter space in our model, there are several real-world processes missing from our model that make it implausible that slowing test returns would actually be an effective public health measure. First, our model is missing the components that would allow us to model the primary benefit of rapid testing, i.e. detecting and containing outbreaks while they are still in progress. This process could be modeled phenomenologically by making the testing focus an increasing function of the speed of test returns (i.e. $\partial w_I(\omega)/\partial\omega > 0$), because rapid testing allows more tests to be concentrated on infected individuals. Second, in the real world individuals become less likely to maintain isolation if they are required to do so for longer; phenomenologically, we could allow effectiveness of isolation while waiting for test returns an increasing function of test return speed ($\partial\theta_W(\omega)/\partial\omega > 0$), or we could introduce a separate "waiting, but no longer isolating" compartment that individuals entered from the "waiting, isolated" compartment at a specified rate. Third and finally, if one wants to decrease the overall transmission rate of the population there are more effective methods than keeping tested people in limbo: masking, ventilation, distancing measures, retail and event closures, stay-at-home orders, ...

The other counterintuitive result from our analysis is that, for sufficiently high testing intensity ρ, increasing testing intensity can actually increase $\mathcal{R}_0$ (e.g. Fig. 3(b), upper right panel [$\theta_c = 1$, $\theta_w = 0$]). This phenomenon occurs mainly because of a peculiar feature of the DFE in our model: we assume that testing is ongoing before the beginning of the epidemic, so that the starting point of the epidemic invasion is an equilibrium distribution of susceptibles between the S_{n} (untested) and S_{u} (waiting) compartments: in particular, $S_{\mathrm{u}}^* = \rho/(\rho+\omega)$. (In reality, testing intensity itself is a dynamic variable that will increase as the epidemic proceeds.) If isolation in the waiting compartment is low ($\theta_w \ll 1$), then waiting individuals can easily be infected once the epidemic starts. Once infected they can still infect others while in the waiting compartment, and cannot be tested again before they have returned to the untested compartment. Thus, under certain extreme conditions (low θ_w, high θ_c, low ω, high ρ), $\mathcal{R}_0$ becomes an increasing function of testing intensity. [**BMB:** *This phenomenon*

occurs primarily (only??) for targeted testing, because ... CAN WE FIGURE OUT WHY? Targeting should be irrelevant to determining the DFE (because everyone is S at that point), so what is the dynamical explanation? Is there a second order effect somewhere, e.g. testing is more effective overall (darker colours in Fig 3(b) upper-right panel than in Fig 3(a) upper panel), so we more quickly reach the point where the effect of increasing S_n^* outweighs the beneficial effects of testing?] However, this phenomenon is even more unrealistic than the possibility that slowing test returns increases $\mathcal{R}_0$. It depends both on the assumption that regular testing is occurring before the epidemic starts, and on levels of testing that are unrealistically high (at least in large, general-population settings), i.e. at least 10% of the population being tested per day.

Although we model the testing process in more detail than most mathematically focused epidemiological models, one place where more detail could be informative is in the processes determining the testing weights $\{w_S, w_I, w_R\}$. While random testing, as done for surveillance purposes, unambiguously leads to equal testing weights, making precise quantitative connections between public health practices and testing weights is difficult in other contexts. The testing weights reflect the correlation between an individual's risk of infection and their likelihood of being tested due to age, occupation, geographic location, etc.. This correlation is influenced, among many other factors, by the proportion of the uninfected population with COVID-like symptoms (e.g. due to seasonal upper respiratory tract infections); the concentration of transmission and testing in hot spots such as long-term care facilities and high-density workplaces; the overall testing intensity (and hence e.g. restriction to symptomatic individuals); and the proportion of COVID-infected people who are symptomatic. Future steps should explore mathematically tractable ways to model some of these factors more precisely. For example, separating the infected class into exposed, symptomatic, and a- or pre-symptomatic compartments and allowing the testing weights to vary across non-symptomatic (exposed/asymptomatic/presymptomatic) vs. symptomatic compartments could reflect the allocation of tests to diagnostic purposes (targeting symptomatic individuals) vs. contact-tracing (targeting infected but non-symptomatic individuals) vs. screening (relatively equal weights, depending on the venue). Alternatively, one could make the testing weights depend on the testing intensity or test return rate as suggested above. Whatever complexity is added would probably put the model beyond reach of the analytical methods we have used in this paper, but one could still use semi-numerical methods such as constructing the next-generation matrix and using it to evaluate the derivatives of $\mathcal{R}_0$ with respect to the parameters numerically.

Although testing and tracing is a key part of infection control strategy, mathematical epidemiologists have typically analyzed it with detailed models designed to inform particular public health efforts, rather than analyzing simple but general models of the feedback between testing and epidemic dynamics [**BMB:** *can we back this statement up? more general citations to test-and-trace? HIV? Bergstrom et al might be a counterexample, although it's for a different context [repeated testing of an isolated population]*]. We hope that this paper will inspire further explorations of the fundamental properties of dynamical systems that incorporate explicit testing models in an epidemiological context. [**BMB:** *we could also talk about test and trace as a 'speed' intervention, but I'm tired*].

[**BMB:** *Leftover comments:*

- *should emphasize (at some appropriate point in text) that Δ is independent of β (and hence of $\mathcal{R}_0$ if we are thinking primarily of holding γ constant and varying β) for the small-ρ (Taylor-expansion) case, see Eq. A22.*

- *it would be good to have a few more testing refs: Bergstrom et al., there might be some other stuff we can recycle from the lab meeting review; Friston's stuff deserves to be mentioned because it does have explicit testing flows too. We should try not to ignore/piss anyone off who has already done stuff*

]

[**Ali:** *This belongs to introduction?*] There have been several modeling works of testing and tracing dynamics and their interaction with epidemiological dynamics. In the context of repeated screaning and random testing of isolated populations (such as a university setup), Bergstrom et al. (2020) provided some analytical results, Rogers et al. (2021) simulated a SEIR model with high-low testing intensity and sensitivity. Further, Friston et al. (2021) model the effects of self-isolation on testing and tracking. Our modeling approache is novel compared to these works.

References

Bergstrom, T., Bergstrom, C. T., and Li, H. (2020). Frequency and accuracy of proactive testing for COVID-19. *medRxiv*.

Dietz, K. (1993). The estimation of the basic reproduction number for infectious diseases. *Statistical methods in medical research*, 2(1):23–41.

Foddai, A., Lubroth, J., and Ellis-Iversen, J. (2020). Base protocol for real time active random surveillance of coronavirus disease (COVID-19)–adapting veterinary methodology to public health. *One Health*, page 100129.

Friston, K. J., Parr, T., Zeidman, P., Razi, A., Flandin, G., Daunizeau, J., Hulme, O. J., Billig, A. J., Litvak, V., Price, C. J., et al. (2021). Testing and tracking in the UK: A dynamic causal modelling study. *Wellcome Open Research*, 5:144.

Kain, M. P., Childs, M. L., Becker, A. D., and Mordecai, E. A. (2021). Chopping the tail: How preventing superspreading can help to maintain COVID-19 control. *Epidemics*, 34:100430.

Keeling, M. J. and Rohani, P. (2011). *Modeling infectious diseases in humans and animals*. Princeton University Press.

Ma, J. and Earn, D. J. D. (2006). Generality of the final size formula for an epidemic of a newly invading infectious disease. *Bulletin of Mathematical Biology*, 68(3):679–702.

Maple (2010). Maplesoft, a division of Waterloo Maple Inc., Waterloo, Ontario. Version 14.

R Core Team (2020). *R: A Language and Environment for Statistical Computing*. R Foundation for Statistical Computing, Vienna, Austria.

Rogers, W., Ruiz-Aravena, M., Hansen, D., Sonoma, W. M., Kessler, M., Fields, M. W., Ferrari, M. J., Chang, C. B., Morrow, J., Hoegh, A., et al. (2021). High-frequency screening combined with diagnostic testing for control of SARS-CoV-2 in high-density settings: an economic evaluation of resources allocation for public health benefit. *medRxiv*.

Shaw, C. L. and Kennedy, D. A. (2021). What the reproductive number R_0 can and cannot tell us about COVID-19 dynamics. *Theoretical Population Biology*.

van den Driessche, P. and Watmough, J. (2002). Reproduction numbers and sub-threshold endemic equilibria for compartmental models of disease transmission. *Mathematical biosciences*, 180(1-2):29–48.

Weitz, J. S., Park, S. W., Eksin, C., and Dushoff, J. (2020). Awareness-driven behavior changes can shift the shape of epidemics away from peaks and toward plateaus, shoulders, and oscillations. *Proceedings of the National Academy of Sciences*, 117(51):32764–32771.

A Appendix

A.1 Model and calculation of $\mathcal{R}_0$

The model in the form of a system of ordinary differential equations is

$$
\begin{aligned}
dS_{\mathrm{u}}/dt &= -\Lambda S_{\mathrm{u}} - F_S S_{\mathrm{u}} + \omega S_{\mathrm{n}}, && \text{(A1a)}\\
dS_{\mathrm{n}}/dt &= -(1-\theta_{\mathrm{w}})\Lambda S_{\mathrm{n}} + (1-p_S)F_S S_{\mathrm{u}} - \omega S_{\mathrm{n}}, && \text{(A1b)}\\
dS_{\mathrm{p}}/dt &= -(1-\theta_{\mathrm{w}})\Lambda S_{\mathrm{p}} + p_S F_S S_{\mathrm{u}} - \omega S_{\mathrm{p}}, && \text{(A1c)}\\
dS_{\mathrm{c}}/dt &= -(1-\theta_{\mathrm{c}})\Lambda S_{\mathrm{c}} + \omega S_{\mathrm{p}}, && \text{(A1d)}\\
dI_{\mathrm{u}}/dt &= \Lambda S_{\mathrm{u}} - F_I I_{\mathrm{u}} + \omega I_{\mathrm{n}} - \gamma I_{\mathrm{u}}, && \text{(A1e)}\\
dI_{\mathrm{n}}/dt &= (1-\theta_{\mathrm{w}})\Lambda S_{\mathrm{n}} + (1-p_I)F_I I_{\mathrm{u}} - \omega I_{\mathrm{n}} - \gamma I_{\mathrm{n}}, && \text{(A1f)}\\
dI_{\mathrm{p}}/dt &= (1-\theta_{\mathrm{w}})\Lambda S_{\mathrm{p}} + p_I F_I I_{\mathrm{u}} - \omega I_{\mathrm{p}} - \gamma I_{\mathrm{p}}, && \text{(A1g)}\\
dI_{\mathrm{c}}/dt &= (1-\theta_{\mathrm{c}})\Lambda S_{\mathrm{c}} + \omega I_{\mathrm{p}} - \gamma I_{\mathrm{c}}, && \text{(A1h)}\\
dR_{\mathrm{u}}/dt &= \gamma I_{\mathrm{u}} - F_R R_{\mathrm{u}} + \omega R_{\mathrm{n}}, && \text{(A1i)}\\
dR_{\mathrm{n}}/dt &= \gamma I_{\mathrm{n}} + (1-p_R)F_R R_{\mathrm{u}} - \omega R_{\mathrm{n}}, && \text{(A1j)}\\
dR_{\mathrm{p}}/dt &= \gamma I_{\mathrm{p}} + p_R F_R R_{\mathrm{u}} - \omega R_{\mathrm{p}}, && \text{(A1k)}\\
dR_{\mathrm{c}}/dt &= \gamma I_{\mathrm{c}} + \omega R_{\mathrm{p}}, && \text{(A1l)}\\
dN/dt &= \omega(S_{\mathrm{n}} + I_{\mathrm{n}} + R_{\mathrm{n}}), && \text{(A1m)}\\
dP/dt &= \omega(I_{\mathrm{p}} + R_{\mathrm{p}}), && \text{(A1n)}
\end{aligned}
$$

(see Table 1 for parameter definitions). The next generation matrix for this model is $G = FV^{-1}$, where matrix F represents the inflow of new infection to the infected compartments and matrix V represents the flow in the infected compartments when the population is totally susceptible. Matrices F and V are

$$
\begin{aligned}
F =& \beta/N_0 \begin{bmatrix} S_{\mathrm{u}}^* & (1-\theta_{\mathrm{w}})S_{\mathrm{u}}^* & (1-\theta_{\mathrm{w}})S_{\mathrm{u}}^* & (1-\theta_{\mathrm{c}})S_{\mathrm{u}}^* \\ (1-\theta_{\mathrm{w}})S_{\mathrm{n}}^* & (1-\theta_{\mathrm{w}})^2 S_{\mathrm{n}}^* & (1-\theta_{\mathrm{w}})^2 S_{\mathrm{n}}^* & (1-\theta_{\mathrm{w}})(1-\theta_{\mathrm{c}})S_{\mathrm{n}}^* \\ 0 & 0 & 0 & 0 \\ 0 & 0 & 0 & 0 \end{bmatrix} && \text{(A2)}\\
=& \beta/N_0 \begin{bmatrix} S_{\mathrm{u}}^* \\ (1-\theta_{\mathrm{w}})S_{\mathrm{n}}^* \\ 0 \\ 0 \end{bmatrix} \begin{bmatrix} 1, 1-\theta_{\mathrm{w}}, 1-\theta_{\mathrm{w}}, 1-\theta_{\mathrm{c}} \end{bmatrix}, \text{and} && \text{(A3)}
\end{aligned}
$$

$$
V = \begin{bmatrix} \hat{F}_I + \gamma & -\omega & 0 & 0 \\ -(1-p_I)\hat{F}_I & \omega+\gamma & 0 & 0 \\ -p_I\hat{F}_I & 0 & \omega+\gamma & 0 \\ 0 & 0 & -\omega & \gamma \end{bmatrix}. \qquad \text{(A4)}
$$

The matrix inverse of V is

$$V^{-1} = \frac{1}{\gamma C}\begin{bmatrix} \gamma(\omega+\gamma)^2 & \gamma\omega(\omega+\gamma) & 0 & 0 \\ \gamma(\omega+\gamma)(1-p_I)\hat{F}_I & \gamma(\omega+\gamma)(\hat{F}_I+\gamma) & 0 & 0 \\ \gamma(\omega+\gamma)p_I\hat{F}_I & \gamma\omega p_I\hat{F}_I & C\gamma/(\omega+\gamma) & 0 \\ \omega(\omega+\gamma)p_I\hat{F}_I & \omega^2 p_I\hat{F}_I & C\omega/(\omega+\gamma) & C \end{bmatrix}, \tag{A5}$$

where $C = \big(\gamma(\omega+\gamma) + (\gamma+\omega p_I)\hat{F}_I\big)(\omega+\gamma)$ and $\hat{F}_I$ is the *per capita* testing rate for the infected people and represented in Eq. (5). Note that all the columns of matrix V^{-1} summ up to $1/\gamma$.

The particular form of F with two rows of zeros at the bottom results in the following blocked form of matrix G.

$$G = \begin{bmatrix} G_{11} & G_{12} \\ 0 & 0 \end{bmatrix}, \tag{A6}$$

where both blocked matrices G_{11} and G_{12} are 2 by 2. Given the upper triangular form of matrix G, the basic reproduction number $\mathcal{R}_0$ (defined as the spectral radius of matrix G) is only determined by the blocked matrix G_{11},

$$G_{11} = \frac{\beta}{\gamma C}\begin{bmatrix} (\omega-\rho)/\omega \\ (1-\theta_{\mathrm{w}})\rho/\omega \end{bmatrix}\begin{bmatrix} 1, 1-\theta_{\mathrm{w}}, 1-\theta_{\mathrm{w}}, 1-\theta_{\mathrm{c}} \end{bmatrix}\begin{bmatrix} \gamma(\omega+\gamma)^2 & \gamma\omega(\omega+\gamma) \\ \gamma(\omega+\gamma)(1-p_I)\hat{F}_I & \gamma(\omega+\gamma)(\hat{F}_I+\gamma) \\ \gamma(\omega+\gamma)p_I\hat{F}_I & \gamma\omega p_I\hat{F}_I \\ \omega(\omega+\gamma)p_I\hat{F}_I & \omega^2 p_I\hat{F}_I \end{bmatrix}. \tag{A7}$$

It is notable that matrix F (A2) has rank one and consequently G_{11} does so. That is G_{11} has only one non-zero eigenvalue which is $\mathcal{R}_0$.

The expression of $\mathcal{R}_0$ has a complicated form with all of the model parameters involved. This expression can be simplified and represented given the specific form of matrix G_{11} (A7). For the purpose of simplicity we present $\mathcal{R}_0$ in the manuscript in terms of expressions C, $C1$ and $C2$, specified in (8).

It remains hard to show that the reproduction number $\mathcal{R}_0$ is decreasing with respect to *per capita* testing intensity, ρ, and the speed of the test return, ω, for the feasible ranges of the parameters, that is

$$\omega > 0, \tag{A8}$$

$$0 \le \rho < \omega, \tag{A9}$$

$$0 \le \theta_{\mathrm{w}} \le \theta_{\mathrm{c}} \le 1, \tag{A10}$$

$$\frac{w_I}{w_S} \ge 1. \tag{A11}$$

In realistic cases the testing rate ρ is very small (i.e., only a small fraction of the population can be tested every day); it is thus reasonable to use a linear approximation of $\mathcal{R}_0$ for $\rho \ll 1$ to analyze the behaviour of $\mathcal{R}_0$ with respect to ω (see section A.3). In the next section we provide an equivalent representation of $\mathcal{R}_0$ in order to show that increasing testing intensity typically decreases $\mathcal{R}_0$.

A.2 More testing intensity may decrease $\mathcal{R}_0$

This section shows that $\frac{\partial \Delta}{\partial \rho}$ can be positive or negative, with Δ defined in Eq. (8), and thus $\frac{\partial \mathcal{R}_0}{\partial \rho} < 0$, where $\mathcal{R}_0$ is given in Eq. (6). We rewrite matrix G_{11} in (A7) in the following form to simplify the calculations:

$$G_{11} = \frac{\beta}{\gamma C} \begin{bmatrix} S_{\mathrm{u}}^*/N_0 \\ (1-\theta_{\mathrm{w}})S_{\mathrm{n}}^*/N_0 \end{bmatrix} \begin{bmatrix} C - C_1, C - C_2 \end{bmatrix}, \tag{A12}$$

where C is the same as the one in Eq. (8), i.e.,

$$C = (\omega+\gamma)(\gamma(\omega+\gamma) + (\omega p_I + \gamma)\hat{F}_I),$$

and C_1 and C_2 are

$$\begin{aligned} C_1 =& (\omega+\gamma)(\theta_{\mathrm{w}}\gamma + \theta_{\mathrm{c}}\omega p_I)\hat{F}_I, \\ C_2 =& \big(\omega\gamma(1+p_I)\hat{F}_I + \gamma^2(\omega+\gamma+\hat{F}_I)\big)\theta_{\mathrm{w}} + \omega^2 p_I \hat{F}_I \theta_{\mathrm{c}}, \end{aligned}$$

where $\hat{F}_I$ is given in Eq. (5). Note that for analysis brevity, we let $N_0 = 1$, thus S_{u}^* and S_{n}^* are in the scale of 0 to 1. $\mathcal{R}_0$ is in the same form as in Eq. (6)

$$\mathcal{R}_0 = \frac{\beta}{\gamma}(1-\Delta),$$

where

$$\Delta = \frac{1}{C}\big(C_1 S_{\mathrm{u}}^* + (C_2(1-\theta_{\mathrm{w}}) + C\theta_{\mathrm{w}})S_{\mathrm{n}}^*\big).$$

The first goal is to explore how changes in isolation, θ_{w} and θ_{c}, affects $\mathcal{R}_0$. Mathematically we would like to verify the sign of $\frac{\partial \mathcal{R}_0}{\partial \theta_{\mathrm{w}}}$ and $\frac{\partial \mathcal{R}_0}{\partial \theta_{\mathrm{c}}}$. We start with simplifying Δ (A.2) by factoring θ_{w} and θ_{c} in Eq. (A.2). Thus, Δ can be rewritten as

$$\Delta = \frac{1}{C}\Big(- D_1 S_{\mathrm{n}}^* \boldsymbol{\theta_{\mathrm{w}}^2} + \big(-\omega^2 p_I \hat{F}_I S_{\mathrm{n}}^* \boldsymbol{\theta}_{\mathrm{c}} + D_2 S_{\mathrm{n}}^* + \gamma \hat{F}_I(\omega+\gamma)\big)\boldsymbol{\theta}_{\mathrm{w}} + (\omega + \gamma S_{\mathrm{u}}^*)\omega p_I \hat{F}_I \boldsymbol{\theta}_{\mathrm{c}}\Big), \tag{A13}$$

where

$$D_1 = (\omega+\gamma)\gamma^2 + (\omega+\gamma+\omega p_I)\gamma\hat{F}_I, \tag{A14}$$

$$D_2 = (3\omega+2\gamma)\gamma^2 + (\omega+\gamma+2\omega p_I)\gamma\hat{F}_I + (\gamma + p_I\hat{F}_I)\omega^2. \tag{A15}$$

Δ, Eq. (A13), is linear in θ_{c} with a positive coefficient. thus

$$\frac{\partial \Delta}{\partial \theta_{\mathrm{c}}} = 1/C(\gamma S_{\mathrm{u}}^* + \omega(1-\theta_{\mathrm{w}}S_{\mathrm{n}}^*))\omega p_I \hat{F}_I. \tag{A16}$$

This results in increasing Δ, thus decreasing $\mathcal{R}_0$ with respect to θ_{c}, that is $\frac{\partial \mathcal{R}_0}{\partial \theta_{\mathrm{c}}} \leq 0$. Note that C is independent of θ_{c} and θ_{w}.

With a similar logic, Δ (A13) is a concave-down quadratic equation in θ_{w}, given by

$$1/C\Big(- D_1 S_{\mathrm{n}}^* \boldsymbol{\theta_{\mathrm{w}}^2} + \big(-\omega^2 p_I \hat{F}_I S_{\mathrm{n}}^* \boldsymbol{\theta}_{\mathrm{c}} + D_2 S_{\mathrm{n}}^* + \gamma \hat{F}_I(\omega+\gamma)\big)\boldsymbol{\theta}_{\mathrm{w}}\Big). \tag{A17}$$

We show that the feasible range of θ_{w} lies between 0 and the vertex of this parabola where the parabola is increasing in θ_{w}, and so does Δ which results in inferring $\frac{\partial \mathcal{R}_0}{\partial \theta_{\mathrm{w}}} \leq 0$. It is enough to show that partial derivative of the expression (A17) with respect to θ_{w} at $\theta_{\mathrm{w}} = 1$ is non-negative. It follows that

$$\begin{aligned}\left.\frac{\partial \Delta}{\partial \theta_{\mathrm{w}}}\right|_{\theta_{\mathrm{w}}=1} =& 1/C\Big((D_2 - 2D_1 - \omega^2 p_I \hat{F}_I \theta_{\mathrm{c}}) S^*_{\mathrm{n}} + \gamma \hat{F}_I(\omega+\gamma)\Big) \\ =& 1/C\Big((\gamma(\omega+\gamma) + \gamma\omega^2 + (1-\theta_{\mathrm{c}})\omega^2 p_I \hat{F}_I) S^*_{\mathrm{n}} + \gamma(\omega+\gamma)\hat{F}_I(1 - S^*_{\mathrm{n}})\Big),\end{aligned} \tag{A18}$$

which is a positive quantity, given that θ_{c} and S^*_{n} vary between 0 and 1.

The second goal is to explore how changes in *per capita* testing intensity ρ affects $\mathcal{R}_0$. Mathematically we would like to verify the sign of $\frac{\partial \mathcal{R}_0}{\partial \rho}$, which specifically depends on $\frac{\partial \Delta}{\partial \rho}$. We use the derived expressions for S^*_{u} and S^*_{n}, given by Eqs. (4), in Δ (A.2). Also, we define $\phi = \hat{F}_S = \frac{\rho\omega}{\omega - \rho}$, to reparameterize ρ. This is mainly to avoid singularity in $\hat{F}_I$ (5), when testing intensity ρ is very close to the rate of test return ω. Thus, ρ is reparameterized as

$$\rho = \frac{\omega\phi}{\omega + \phi}. \tag{A19}$$

This one-to-one monotonic reparameterization enables us to simplify the mathematical expressions and explore the simpler $\frac{\partial \Delta}{\partial \phi}$ instead of the complicated $\frac{\partial \Delta}{\partial \rho}$. The derivative is

$$\partial\Delta/\partial\phi = \frac{1}{d_3}(a_3\phi^2 + b_3\phi + c_3), \tag{A20}$$

where

$$\begin{aligned} a_3 = \frac{w_I}{w_S}\Bigg(& (1-\theta_{\mathrm{w}})(1+\frac{w_I}{w_S})\theta_{\mathrm{w}}\gamma^3 + (1-\theta_{\mathrm{c}})p_I^2\theta_{\mathrm{w}}\frac{w_I}{w_S}\omega^3 \\ & + \Big(\big((1-\theta_{\mathrm{w}} - \frac{w_I}{w_S})\theta_{\mathrm{c}} + (3-2\theta_{\mathrm{w}})\theta_{\mathrm{w}}\frac{w_I}{w_S}\big)p_I + (1-\theta_{\mathrm{w}})(1+\frac{w_I}{w_S})\theta_{\mathrm{w}}\Big)\omega\gamma^2 \\ & + \Big(\big((1-\theta_{\mathrm{w}} - \theta_{\mathrm{w}}\frac{w_I}{w_S})\theta_{\mathrm{c}} + (2-\theta_{\mathrm{w}})\theta_{\mathrm{w}}\frac{w_I}{w_S}\big)p_I + (2\theta_{\mathrm{w}} - \theta_{\mathrm{w}}^2 - \theta_{\mathrm{c}})\frac{w_I}{w_S}p_I^2\Big)\omega^2\gamma\Bigg), \\ b_3 = & \ 2\frac{w_I}{w_S}(\omega+\gamma)\gamma\Big((\omega+\gamma+\omega p_I)(2-\theta_{\mathrm{w}})\gamma\theta_{\mathrm{w}} + (1-\theta_{\mathrm{w}})\omega^2 p_I\theta_{\mathrm{c}} + \omega^2 p_I\theta_{\mathrm{w}}\Big), \\ c_3 = & \ (\omega+\gamma)^2\gamma\Big((2-\theta_{\mathrm{w}})\gamma^2\theta_{\mathrm{w}} + (1+\frac{w_I}{w_S})\omega\gamma\theta_{\mathrm{w}} + \frac{w_I}{w_S}\omega^2 p_I\theta_{\mathrm{c}}\Big), \\ d_3 = & \ \frac{(\omega+\gamma)}{\omega}\Big((\omega p_I + \gamma)\frac{w_I}{w_S}\phi + (\omega+\gamma)\gamma\Big)^2(\omega+\phi)^2. \end{aligned} \tag{A21}$$

Note that $\phi \geq 0$, also b_3, c_3 and d_3 are all positive. However a_3 can be positive or negative. If $a_3 \geq 0$, $\partial\Delta/\partial\phi \geq 0$ for all feasible range of parameters, thus $\frac{\partial \mathcal{R}_0}{\partial \rho} \leq 0$. It is straight forward to show that $a_3 \geq 0$ in case of random testing strategy, i.e., $w_{\mathrm{S}} = w_{\mathrm{I}} = 1$. If $a_3 < 0$, then the quadratic expression in the numerator of (A20) has a positive root, ϕ^*, such that for $\phi > \phi^*$, $\partial\Delta/\partial\phi < 0$.

An example of this counter-vailing effect of ϕ, and consequently ρ, on $\mathcal{R}_0$ occurs when $\theta_{\rm w} = 0$ and $\theta_{\rm c} = 1$. This is illustrated in the top-right panel of the Fig. 3 panel (b), where the strength of isolation for awaiting people is the least, but the most for the confirmed cases. In this case, simplifying a_3 in Eq. (A21) gives

$$a_3 = \frac{w_I}{w_S}\omega\gamma p_I((\omega+\gamma) - \frac{w_I}{w_S}(\omega p_I + \gamma)).$$

Specifically, in the case of targeted testing which is identified by $\frac{w_I}{w_S} > 1$, and using a perfect sensitive test, thus $p_I = 1$, there exists a range for ρ over which $\frac{\partial \mathcal{R}_0}{\partial \rho} \leq 0$. Note that ρ and ω have a similar mechanism in delaying people to get into $I_{\rm c}$, thus we would expect to see the non-trivial counter-vailing effect of these two parameters on $\mathcal{R}_0$.

A.3 rate of returning tests

The third goal is to explore how changes in the rate of test return ω affects $\mathcal{R}_0$. Mathematically we would like to verify the sign of $\frac{\partial \mathcal{R}_0}{\partial \omega}$, which specifically depends on $\frac{\partial \Delta}{\partial \omega}$. We use the linearization of Δ around $\rho = 0$ to show that there a non-monotonic relationship between $\mathcal{R}_0$ and ω. The linear term in the Taylor expansion of Δ at $\rho = 0$ is

$$\Delta = \frac{\rho}{\omega\gamma(\omega+\gamma)}\Big(\frac{w_I}{w_S}\omega^2 p_I\theta_{\rm c} + (\frac{w_I}{w_S}+1)\gamma\omega\theta_{\rm w} + \gamma^2\theta_{\rm w}(2-\theta_{\rm w})\Big). \tag{A22}$$

This results in

$$\frac{\partial \Delta}{\partial \omega} = \frac{\rho}{\omega^2(\omega+\gamma)^2}\Big((p_I\frac{w_I}{w_S}\theta_{\rm c} - (1+\frac{w_I}{w_S})\theta_{\rm w})\omega^2 + 2\theta_w\gamma(\theta_w - 2)\omega + \theta_w\gamma^2(\theta_w - 2)\Big), \tag{A23}$$

around $\rho = 0$.

A.4 On Testing Rate and Numerical Singularity

In this work, we didn't do any numerical solutions for the trajectories in our analysis. However, if one tries to do so there would be a singularity issue to deal with. Specifically, the numerical singularity issue with the chosen σ (1) is that the population in S compartments appeared to blow up when the DFE is achieved. This is once the only untested people are susceptibles, the FOI will become $\Lambda = 0$, testing rate $F_s = \rho N_0/S_{\rm u}$. Thus, the first equation of the model (A1) will become $dS_{\rm u}/dt = -\rho N_0 + \omega S_{\rm n}$. Thus changes in $S_{\rm u}$ will be no longer dependent on $S_{\rm u}$ with a linear rate of leaving the $S_{\rm u}$ compartment. IN fact the testing rate, σ, should be formulated such that people from the untested compartments will not be tested if they are not there. One way to fix this issue, is to consider a maximum testing rate, τ (1/day). In general, we want to test at a rate of ρ across the whole population. This won't always be possible, so we impose a maximum rate of τ per testable person and redefine $\sigma = \frac{\tau\rho N_0}{\tau W + \rho N_0}$, with the assumption that $\tau \gg \rho$. This alteration in σ, does not change any results related to $\mathcal{R}_0$, thus we only impose it in the simulation of the epidemic dynamic.

A.5 The effect of testing focus parameter $\frac{w_I}{w_S}$ on $\mathcal{R}_0$

We define $w_{\mathrm{IS}} = \frac{w_I}{w_S}$.

$$\frac{\partial \Delta}{\partial w_{\mathrm{IS}}} = \frac{(\omega-\rho)(\omega(\omega-\rho\theta_{\mathrm{w}})+\gamma(\omega-\rho))(\theta_{\mathrm{w}}\gamma+\theta_{\mathrm{c}}\omega p_{\mathrm{I}})}{(-\omega^2\gamma+\omega\gamma\rho-\gamma\rho\omega w_{\mathrm{IS}}-\omega\gamma^2+\gamma^2\rho-\omega^2 p_I\rho w_{\mathrm{IS}})^2}, \tag{A24}$$

which is a positive quantity. Thus, $\frac{\partial \mathcal{R}_0}{\partial w_{\mathrm{IS}}} \leq 0$. Therefore, increasing the focus of testing on the infectious people will result in less transmission.